APPLIED AND ENVIRONMENTAL MICROBIOLOGY, Jan. 2006, p. 890–900 Vol. 72, No. 1
0099-2240/06/$08.00+0 doi:10.1128/AEM.72.1.890–900.2006

Cellular Response of *Shewanella oneidensis* to Strontium Stress†

Steven D. Brown,[1] Madhavi Martin,[1] Sameer Deshpande,[2] Sudipta Seal,[2] Katherine Huang,[3,4] Eric Alm,[3,4] Yunfeng Yang,[1] Liyou Wu,[1] Tingfen Yan,[1] Xueduan Liu,[1]‡ Adam Arkin,[3,5] Karuna Chourey,[1] Jizhong Zhou,[1,4] and Dorothea K. Thompson[1,4]*

Environmental Sciences Division, Oak Ridge National Laboratory, Oak Ridge, Tennessee 37831[1]; Advanced Materials Processing and Analysis Center, Materials and Aerospace Engineering, University of Central Florida, Orlando, Florida 32816[2]; Department of Bioengineering, University of California, Berkeley, California 94720[3]; Virtual Institute for Microbial Stress and Survival[4]§; and Physical Biosciences Division, Lawrence Berkeley National Laboratory, Berkeley, California 94720[5]

Received 30 June 2005/Accepted 2 November 2005

The physiology and transcriptome dynamics of the metal ion-reducing bacterium *Shewanella oneidensis* strain MR-1 in response to nonradioactive strontium (Sr) exposure were investigated. Studies indicated that MR-1 was able to grow aerobically in complex medium in the presence of 180 mM $SrCl_2$ but showed severe growth inhibition at levels above that concentration. Temporal gene expression profiles were generated from aerobically grown, mid-exponential-phase MR-1 cells shocked with 180 mM $SrCl_2$ and analyzed for significant differences in mRNA abundance with reference to data for nonstressed MR-1 cells. Genes with annotated functions in siderophore biosynthesis and iron transport were among the most highly induced (>100-fold [$P < 0.05$]) open reading frames in response to acute Sr stress, and a mutant (SO3032::pKNOCK) defective in siderophore production was found to be hypersensitive to $SrCl_2$ exposure, compared to parental and wild-type strains. Transcripts encoding multidrug and heavy metal efflux pumps, proteins involved in osmotic adaptation, sulfate ABC transporters, and assimilative sulfur metabolism enzymes also were differentially expressed following Sr exposure but at levels that were several orders of magnitude lower than those for iron transport genes. Precipitate formation was observed during aerobic growth of MR-1 in broth cultures amended with 50, 100, or 150 mM $SrCl_2$ but not in cultures of the SO3032::pKNOCK mutant or in the abiotic control. Chemical analysis of this precipitate using laser-induced breakdown spectroscopy and static secondary ion mass spectrometry indicated extracellular solid-phase sequestration of Sr, with at least a portion of the heavy metal associated with carbonate phases.

The toxic heavy metal and radionuclide waste derived from defense-related activities and various industrial processes can seriously impact the health of ecosystems and humans. In situ bioremediation exploiting the intrinsic respiratory processes of dissimilatory metal ion-reducing bacteria (DMRB) has been proposed as a potential strategy for the reductive immobilization or detoxification of environmental contaminants. Microbial cell walls, for example, can serve as templates for nucleation of metal precipitates (4), and metal-reducing bacteria can directly convert metal pollutants from a soluble, mobile form to a sparingly soluble, less bioavailable form (28), thus facilitating contaminant removal from contained-storage and natural sites. Microbially mediated immobilization of toxic metals and radionuclides can occur as a result of precipitation through formation of metal-metabolite/ligand complexes, nonenzymatic biosorption, or bioaccumulation by energy-dependent transport systems (reviewed in references 4, 13, and 27). However, the application of DMRB to contaminated sites is often complicated by the unpredictability of individual microbial processes and by complex interspecies interactions, as well as by fluctuations in environmental conditions (e.g., local pH, metal toxicity, and water availability).

Among DMRB, members of the genus *Shewanella* comprise a major group of environmental gamma proteobacteria that have been investigated largely from the perspectives of ecology, physiology, and biochemistry until recently. *Shewanella oneidensis* strain MR-1 possesses remarkable metabolic versatility with respect to electron acceptor utilization; for example, it can use oxygen, nitrate, fumarate, Fe(III), Mn(III) and (IV), Cr(VI), and U(VI) as terminal electron acceptors during respiration (26, 32–36). Because of its metabolic versatility and potential for serving as a model environmental microorganism, the complete DNA sequence of the *S. oneidensis* MR-1 genome has been determined (18), and the genomes of an additional 14 *Shewanella* species have been targeted for sequencing by the U.S. Department of Energy (DOE) Joint Genome Institute.

Strontium (Sr) is found in the environment in a variety of different compounds and is chemically analogous to calcium; hence, there is a tendency for Sr to be incorporated into bone (31, 48). The divalent cation Sr^{2+} is a common groundwater contaminant present at various DOE field sites, including the Natural and Accelerated Bioremediation Research (NABIR) Field Research Center (FRC) at Oak Ridge National Laboratory (see the website http://www.esd.ornl.gov/nabirfrc/index.html). *Shewanella* spp., as well as Fe(III) oxide and bacteria

* Corresponding author. Present address: Department of Biological Sciences, Purdue University, 1-118 Lilly Hall of Life Sciences, 915 West State Street, West Lafayette, IN 47907-2054. Phone: (765) 496-8301. Fax: (765) 494-0876. E-mail: dthomps@purdue.edu.

† Supplemental material for this article may be found at http://aem.asm.org/.

‡ Present address: School of Minerals Processing and Bioengineering, Central South University, Changsha, Hunan, People's Republic of China 410083.

§ http://vimss.lbl.gov.

coated with Fe(III) oxides, have been shown to sorb Sr^{2+}, thus affecting the fate and transport of such inorganic contaminants in natural aqueous environments (15, 45, 46). However, very little is known about the cellular response of *Shewanella* species to toxic concentrations of heavy metals at the molecular level.

In this study, we determined global alterations in the temporal transcriptional profiles of *S. oneidensis* MR-1 following acute $SrCl_2$ exposure to understand the cellular response to nonradioactive Sr stress. Time series microarray experiments suggested that genes with annotated functions in siderophore biosynthesis and iron transport played an important role in the cellular response to Sr. A mutant strain defective in siderophore biosynthesis was hypersensitive to $SrCl_2$, and liquid cultures of this mutant did not support precipitate formation, in contrast to cultures of parental and wild-type strains. High-resolution spectrometry techniques indicated that a significant portion of the Sr was captured in solid-phase compounds, such as carbonate, formed during aerobic growth of MR-1 in complex medium amended with $SrCl_2$.

MATERIALS AND METHODS

Bacterial strains, plasmids, and growth conditions. *S. oneidensis* strain MR-1 (33) was used for growth and microarray hybridization experiments. *S. oneidensis* strain DSP10 (50), a spontaneous rifampin derivative of MR-1, was used to construct pKNOCK insertion mutants, with *Escherichia coli* S17-1/λ_{pir} (21) as the donor strain. *S. oneidensis* and *E. coli* were grown in Luria-Bertani (LB) medium (42) at 30°C and 37°C, respectively. Antibiotics were added to the growth media at the following concentrations: for *E. coli*, kanamycin (Km) at 50 μg/ml; and for *S. oneidensis*, rifampin at 10 μg/ml and Km at 25 μg/ml. For time series microarray hybridization experiments, *S. oneidensis* MR-1 was grown aerobically in LB medium and then challenged with 180 mM $SrCl_2$ (Sigma-Aldrich Co., St. Louis, MO) or allowed to continue growing in the absence of $SrCl_2$ at 30°C with shaking at 250 rpm in a New Brunswick Scientific (Edison, NJ) incubator.

Generation of insertion mutants. *S. oneidensis* genes SO3032 and SO3034 were disrupted by integration of the suicide plasmid pKNOCK-Km^r essentially as described previously (50). The suicide plasmid pKNOCK-Km^r has been described elsewhere (1). Briefly, an internal fragment for each gene (223 bp, SO3032; 194 bp, SO3034) was amplified by PCR using the following primer sets: for SO3032, 3032F (5′-CATCACACCACAGATTTACG-3′) and 3032R (5′-CAAGAGGGTTTCACTTATGC-3′); and for SO3034, 3034F (5′-CGCATTTAACGACAACG-3′) and 3034R (5′-CAAGAGGGTTTCACTTATGC-3′). The purified PCR products were ligated into the SmaI site of pKNOCK-Km^r, and the resulting plasmids were introduced into competent *E. coli* S17-1/λ_{pir} cells by electroporation. The SO3032::pKNOCK-Km^r and SO3034::pKNOCK-Km^r plasmids were then mobilized from their *E. coli* hosts into *S. oneidensis* DSP10 in biparental matings. Insertional mutants were confirmed by PCR amplification using a combination of plasmid-specific primers and primers complementary to chromosomal DNA sequences that flanked the target gene but were not complementary to sequences within the original amplicon. These primer sequences were the following: internal pKNOCK primer KS (5′-TCGAGGTCGACGGTATCG-3′), SK (5′-GGATCCACTAGTTCTAGAGCG-3′), or KS reverse complement (5′-GATACCGTCGACCTCGA-3′), depending on the orientation of the cloned PCR product; and outside primers 3032O (5′-TGAGTTTACCCATGAGAAGC-3′) and 3034O (5′-GCTGAAATCATCCACTCG-3′), which flanked the SO3032::pKNOCK-Km^r and SO3034::pKNOCK-Km^r insertions, respectively. The PCR primers 3032A (5′-GTAGGTGAGCCGATGAACTT-3′) and 3032B (5′-GTGTGATGGCAAGTGGGTAG-3′) annealed to DNA sequences located 5′ and 3′, respectively, of the SO3032 gene and were also used to confirm the integration of the pKNOCK suicide plasmid at the appropriate locus.

Characterization of MR-1 and mutant growth in the presence of Sr. Inocula were prepared by growing strains overnight (16 to 20 h) in LB medium with antibiotic as appropriate, followed by diluting them 1:1,000 into LB media that contained different $SrCl_2$ concentrations and lacked antibiotic. MR-1 sensitivity to $SrCl_2$ was determined by culturing the strain in 5 ml of Sr-containing medium at 30°C in glass tubes with shaking at 250 rpm for 48 h. Culture turbidity (optical density at 600 nm [OD_{600}]) was measured by using a Spectronic 20D+ spectrophotometer (Thermo Electron Cooperation, Waltham, MA). Mutant strains were prepared and diluted in a manner similar to that used for MR-1, with the exception that growth was measured in triplicate in a 200-well format using a Bioscreen C system (Labsystems, Franklin, MA). Briefly, 400-μl aliquots of each culture were added to the Bioscreen C wells and grown for 48 h at 30°C with extra intensive shaking, and the OD_{600} was determined every 30 min. SigmaPlot version 8.0 (SPSS Inc., Chicago, IL) was used to plot growth curves.

RNA isolation and preparation of fluorescein-labeled cDNA. For time series microarray hybridizations, an overnight culture (16 h) was used to inoculate prewarmed medium in 250-ml sidearm Pyrex flasks. Six cultures were grown aerobically to mid-exponential phase (OD_{600}, 0.5) from an initial OD_{600} of ca. 0.025, and then prewarmed $SrCl_2$ was added to three of the flasks, giving a final concentration of 180 mM in a total volume of 25 ml. The same volume of prewarmed sterile water was added to each of the three remaining control cultures. Cells were harvested for RNA extraction at 5, 30, 60, and 90 min after treatment. To prevent RNA degradation, the cells were washed once with ice-cold LB medium by centrifugation at maximum speed in a 5415R centrifuge (Eppendorf, Westbury, N.Y.) for 20 s at 4°C.

TRIzol reagent (Invitrogen, Carlsbad, CA) was used to isolate total cellular RNA, which was then treated with RNase-free DNase I (Ambion, Texas) to digest residual chromosomal DNA and subsequently purified with a QIAGEN RNeasy Mini kit according to the manufacturer's instructions. Total cellular RNA was quantified at OD_{260} and OD_{280} with a NanoDrop ND-1000 spectrophotometer (NanoDrop Technologies, Wilmington, DE). The purified RNA from each sample served as the template to generate cDNA copies labeled with either Cy3-dUTP or Cy5-dUTP (Amersham Biosciences, Piscataway, NJ). In a duplicate set of cDNA synthesis reactions, the fluorescent dyes were reversed for each sample to minimize artificial dye-specific effects. Labeling reaction components and incubation conditions as well as cDNA probe purification and concentration determination have been described previously (50).

Microarray hybridization, scanning, image quantification, and data analyses. *S. oneidensis* MR-1 microarrays were constructed as described previously (14, 51), with the exception that the arrays were printed on Corning UltraGAPS coated slides (Corning, Corning, NY) using a *Micro*Grid II robotic arrayer (Matrix Technologies, Hudson, NH). Gene expression analysis was performed using six independent microarray experiments (2 dye-swap experiments × 3 biological replicates), with each slide containing two spots for each gene at different locations. The two separately labeled cDNA pools to be compared (i.e., the $SrCl_2$-treated and control samples) were combined in a hybridization solution containing 50% (vol/vol) formamide. Microarray prehybridization, hybridization, and posthybridization washings were carried out according to the manufacturer's instructions, except that prehybridizations and hybridizations were performed at 50°C. The arrays were scanned as described previously (50). The microarray images were quantified using ImaGene version 5.5 (Biodiscovery, Inc., Los Angeles, CA), and the data were transformed and normalized with GeneSite Light (Biodiscovery, Inc.). ArrayStat (Imaging Research, Inc., Ontario, Canada) was used to determine the common error of these values and remove outliers and for analysis of statistical significance via a *z* test for two independent conditions and the false-discovery-rate method. Genes displaying a statistically significant change ($P < 0.05$) in expression ratio with a magnitude change of ≥2-fold were further considered (43). Cluster analysis of the microarray data set was performed using the program Hierarchical Clustering Explorer Version 3.0 (http://www.cs.umd.edu/hcil/multi-cluster/).

Real-time RT-PCR analysis. Microarray data were validated using real-time quantitative reverse transcription-PCR (RT-PCR) as described previously (51), except iQ SYBR green supermix (Bio-Rad, Hercules, Calif.) was used according to the manufacturer's instructions instead of SYBR green I. Four genes were selected for real-time RT-PCR analysis for the 30-, 60-, and 90-min post-$SrCl_2$ samples; these genes represented a range of array expression ratios in response to the $SrCl_2$ treatment from highly repressed to highly induced. The following genes were selected for comparative RT-PCR analysis, and primer pairs (given in parentheses) were designed using the program Primer3 (http://www-genome.wi.mit.edu/cgi-bin/primer/primer3_www.cgi): SO3032 (5′-GATTCTATCCGAGTCACCAG, 3′-CAAGAGGGTTTCACTTATGC), *hmuV* (5′-CACTGTGATTGTGGTATTGC, 3′-AGGTGTAGGTTCACTGACGA), SO3062 (5′-CTACTCTGTGAGCTTGGGTT, 3′-AGCAGAAGTGATAGGCCC), and SO0403 (5′-CGACTCGACGATCAATTTAC, 3′-TGGGTTATAGAAACGACCAC).

LIBS. Solid (precipitate) and liquid phases of *S. oneidensis* MR-1 cultures grown in the presence of 50 mM $SrCl_2$ were subjected to laser-induced breakdown spectroscopy (LIBS) analysis (30) with a Big Sky laser (model Ultra 532; Big Sky Laser Technologies, Inc., Bozeman, MT). This Q-switched Nd-yttrium aluminum garnate laser has an output wavelength of 532 nm, which has a maximum beam energy of 50 mJ per pulse. The laser pulse width is 5 ns, and the repetition rate can vary from 1 to 20 Hz. When operated at a repetition rate of

2 Hz, all the processes, including plasma formation, optical emission, gated detection, data collection, and analysis, were completed within 500 milliseconds, before the next pulse arrived at the sample.

For LIBS analysis, the cell-free medium from MR-1 cell suspensions was obtained by centrifugation (13,000 rpm for 3 min), and the solid-phase material, which included the cells (pinkish color) and extracellular precipitate (white), was washed several times with Milli-Q water. The liquid culture medium (0.2 ml), uninoculated medium (0.2 ml), and solid-phase material in 0.2 ml of Milli-Q water were air dried on separate Whatman 40 filters (4.25 cm in diameter) for 48 h. A Catalina Scientific spectrometer (SE200A; Catalina Scientific Corp., Tucson, AZ) was used to collect light emitted from plasma sparks following laser ablation of samples. The time-resolved spectrum was detected by an intensified charge-coupled device built by Andor Technology (South Windsor, CT), with the intensified charge-coupled device delayed and gated by a delay generator that is integrated onto the detector head. KestrelSpec software (Catalina Scientific Corporation) was used to acquire the emission spectra, identify the peaks, calculate the full width at half-maximum of the peaks of interest, and calculate the area under the peak, which can be used in the semiquantification of elements from a similar matrix.

SIMS. In secondary ion mass spectrometry (SIMS), an incident beam is used to bombard a sample surface, resulting in the desorption of surface species. The sputtered ion species, which range from electrons to atoms and molecules in either the neutral or the ionized state, are electrostatically focused into a mass analyzer for mass-to-charge separation and surface species detection (see reference 5 for a detailed review).

For sample preparation, *S. oneidensis* MR-1 cells were grown as described above in 50 mM or 150 mM $SrCl_2$ or in the absence of $SrCl_2$ (control) for 24 h. Cells were freeze-dried essentially as described previously (29). Briefly, cells were harvested by centrifugation (4,000 rpm for 3 min), and the supernatant was discarded. The cell pellet was resuspended in sodium bicarbonate buffer (2.5 g of sodium bicarbonate/liter) and centrifuged as described above. The cell pellet was resuspended in fresh buffer and supplemented with an equal volume of sodium bicarbonate buffer containing 24% (wt/vol) sucrose. The cell suspension was then frozen in an ethanol-dry ice bath and dried overnight in 1.5-ml Eppendorf tubes. The freeze-dried cells were kept at room temperature.

Static SIMS data were collected for pure $SrCl_2$ (reference sample) and for untreated and $SrCl_2$-treated MR-1 cells using an ADEPT 1010 system (Physical Electronics International, Eden Prairie, MN) at a base pressure of 10^{-8} torr. The SIMS operating beam energy was between 250 eV and 8 keV for oxygen ions but offers full elemental coverage, a sub-part-per-million range sensitivity for most elements, and a spatial resolution of less than 5 μm. In this study, an ion gun was operated with a 3-kV oxygen beam at a 60° take-off angle from the specimen normal. For all data acquisitions, a beam of 2-pA raster was used over an area of 250 mm^2. Peak assignments for quantitative analyses followed the principles described by Eugster et al. (10).

RESULTS

Physiological effect of $SrCl_2$ during aerobic growth. End point culture turbidity determinations were used to assess the physiological effect of various $SrCl_2$ concentrations on aerobic growth of wild-type *S. oneidensis* MR-1. In three independent dose-response experiments, MR-1 was able to grow in the presence of $SrCl_2$ concentrations as high as 180 mM but showed substantial growth inhibition above that concentration (Fig. 1). An $SrCl_2$ concentration of 180 mM was selected for time series gene expression profiling because this dose inhibited cell growth by approximately ≤25% without seriously reducing cell viability.

Transcriptome dynamics of Sr-shocked cells. The global transcriptional response of *S. oneidensis* MR-1 to Sr stress (180 mM $SrCl_2$) was examined based on a time series DNA microarray experiment done at 5, 30, 60, and 90 min postshock with whole-genome microarrays. Temporal gene expression profiles of mid-logarithmic-phase cells challenged with a sublethal concentration of $SrCl_2$ were compared to those of unexposed control cells. A total of 1,806 genes were identified as being significantly differentially expressed ($P < 0.05$) at least at one time point during acute $SrCl_2$ exposure (for complete microarray datasets, see Table S1 in the supplemental material). Pairwise complete-linkage clustering analysis (9) was used to identify suites of genes exhibiting similar or potentially coregulated expression patterns in response to $SrCl_2$ stress. Four major clusters (designated I, II, III, and IV) were observed (Fig. 2).

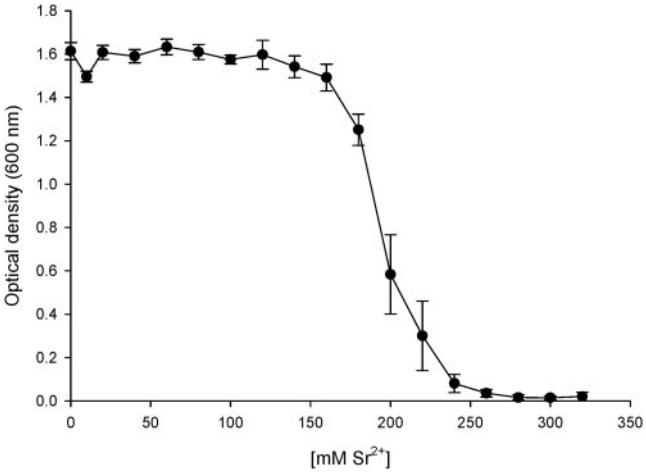

FIG. 1. Dose-response growth curves describing the toxicity of the heavy metal ion Sr^{2+} (as a chloride) on *S. oneidensis* strain MR-1. The MICs were determined in LB broth containing different $SrCl_2$ concentrations under aerobic growth conditions at 30°C by measuring culture turbidity (OD_{600}) in triplicate after 48 h. The graph shows the mean ± standard error (bars) for three independent dose-response curves for wild-type *S. oneidensis* MR-1.

Cluster I (17 genes) contained genes that showed transcriptional up-regulation over the entire exposure period, with induction of expression ratios (*n*-fold) either peaking at the 60-min time point or continuing to increase 90 min following the application of $SrCl_2$ stress (Table 1). Cluster I genes showed the highest increases in expression, which in some cases were greater than 100-fold. The majority (76.5%) of these genes are related to the functional category of transport and binding proteins, as assigned by The Institute for Genomic Research (TIGR; http://www.tigr.org) (Table 2). Three of the other gene products are annotated as hypothetical or conserved hypothetical proteins (the SO3344, SO3667, and SO3668 proteins), and one (the SO4636 protein) is predicted to be a lipoprotein of the cell envelope. Specifically, cluster I was dominated by genes that encode siderophore biosynthesis enzymes, TonB-dependent receptors, and ABC transporters generally involved in iron sequestration and homeostasis (Table 1). Coordinated up-regulation in transcription was observed for a predicted siderophore biosynthesis operon (*alcA*-SO3031-SO3032), a putative operon involved in heme transport (*hugA*-SO3668-SO3667), a TonB1 Fe transport system (*tonB1-exbB1-exbD1*), and a hemin ABC transporter system (*hmuTUV*) (Table 1). Strong candidates for Fur-binding regulatory sites were identified previously in the upstream regions for SO1482 and in the probable *alcA*-SO3031-SO3032, *hugA*-SO3668-SO3667, and *tonB1-exbB1-exbD1* operons by use of computational motif discovery methods (51). Transcript levels for *fur* (SO1937), which encodes the negative regulator of genes involved in sid-

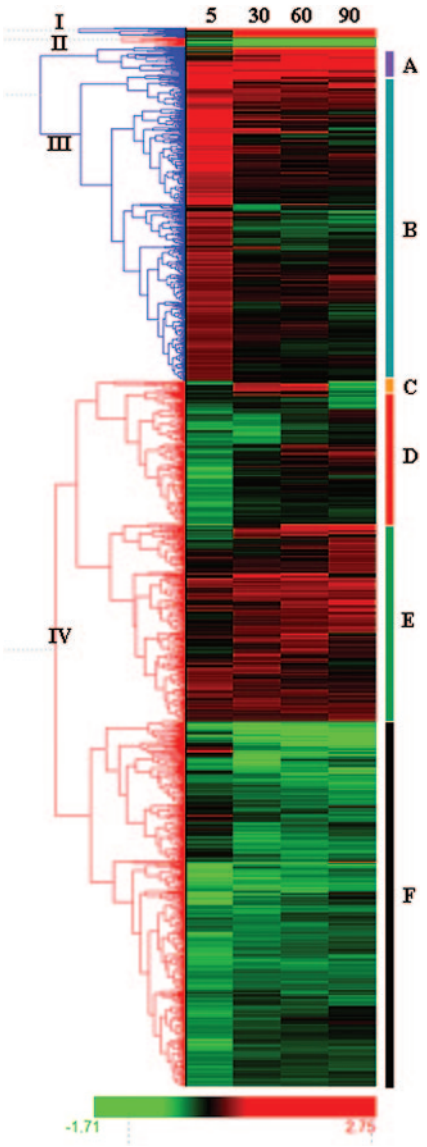

FIG. 2. Complete linkage clustering analysis of 1,806 *S. oneidensis* MR-1 genes exhibiting altered mRNA expression levels in response to exposure to 180 mM $SrCl_2$ over time. Transcriptional profiles are shown at 5, 30, 60, and 90 min after strontium shock. Individual genes are represented by a single row, and each exposure time point is represented by a single column. Red represents induction, while green represents repression. Genes are grouped within four primary clusters (I, II, III, and IV). Subgroups A to F are discussed in the text.

erophore/receptor-mediated iron transport, showed only slight increases (1.2- to 2.2-fold) over the course of the 90-min Sr exposure (see Table S1 in the supplemental material).

In contrast to the temporal expression profiles of cluster I genes, cluster II (14 genes) consisted largely of poorly characterized genes of unknown function (42.6%) that were repressed over the entire 90-min stress period (Fig. 2). Cluster II also contained three genes (SO0101, SO0903, and SO3774) whose products belong to the energy metabolism functional category, as well as two TetR family regulators (SO3627 and SO3743) and one product each assigned to the functional categories of cell envelope (the SO4473 protein), purines/pyrimidines/nucleosides/nucleotides (the SO1258 protein), and unknown functional role (the SO4407 protein).

Cluster III (570 genes) contained genes that displayed different temporal expression patterns in response to $SrCl_2$ (Fig. 2). Genes of subgroup A were typically up-regulated upon strontium stress, although the magnitude of induction was substantially less than that displayed by cluster I genes. For example, genes encoding a putative ferric iron reductase (SO3034), a ferric vibriobactin receptor (*viuA* [SO4516]), and an iron-regulated outer membrane protein (*irgA* [SO4523]) exhibited induction levels of 36-, 29-, and 27-fold, respectively, at the 90-min postshock time point. A putative azoreductase-encoding gene (SO3585), which is potentially involved in cellular detoxification processes, and a sodium:alanine symporter gene (SO3063) showed temporal mean expression ratios of 4.7 (5 min), 2.6 (30 min), 5.2 (60 min), and 5.9 (90 min) and 3.1 (5 min), 2.2 (30 min), 5.8 (60 min), and 9.5 (90 min), respectively. These genes were induced very early (5-min time point) in the exposure period, declined slightly at 30 min, and then increased to even higher levels at the later time points.

Subgroup A also contained genes for various transcriptional regulators (SO2426, SO3684, and SO4524) of undefined function, a putative adenylate cyclase (SO4312), and a sigma-E factor negative regulatory protein (SO1343). According to its gene ontology (18), SO2426 encodes a DNA-binding response regulator, part of a putative two-component signal transduction system. The following increasing transcript levels were measured for gene SO2426 during the entire period of Sr exposure: 1.8 (5 min), 9.8 (30 min), 21 (60 min), and 33 (90 min) (see Table S1 in the supplemental material). Expression of gene SO2426 was also substantially induced in response to iron overload in a *fur* deletion mutant (approximately 30-fold) (51) and hexavalent chromium stress conditions (as much as 11-fold at 90 min after shock) (S. D. Brown et al., unpublished results) and might be part of a two-component signal transduction regulatory system that is involved in sensing and responding to heavy metal toxicity. The involvement of a cognate sensor histidine kinase is not known and cannot be predicted based on the annotated sequence and gene synteny. The other two transcriptional regulators, belonging to the TetR and LysR families of regulators, showed induction levels that ranged from 2.6- to 6.5-fold. This subgroup, which was mostly up-regulated during the entire stress period, also contained approximately threefold more (12.8% of the subgroup) gene products predicted to be involved in protein fate than was annotated in the genome (3.8%) (Table 2).

The remaining genes (255) within cluster III were designated as subgroup B, as the initial induction patterns were similar to those of other members of the cluster but diverged from them considerably after the 5-min time point. Genes in this subgroup coded for either predicted hypothetical or conserved hypothetical proteins representing 48.8% of the subgroup, compared to 39.4% representation of the same functional category across the genome. Putative regulators comprised 6.7% of this subgroup, compared to 4.3% of the genome, as well as genes for 10 signal transduction proteins and sigma-38 (SO3432) and sigma-24 (SO1342) regulatory proteins. Genes showing modestly up-regulated expression (approximately two- to fourfold) early in the $SrCl_2$ exposure period included the following: SO4598 and SOA0153, genes

TABLE 1. Cluster I genes showing high induction (*n*-fold) in response to strontium stress

Gene	Gene product	Mean ratio ($SrCl_2$/control) at[a]:			
		5 min	30 min	60 min	90 min
SO1482	TonB-dependent receptor, putative	0.6	12.8	50.4	52.2
SO3030	Siderophore biosynthesis protein (AlcA)	1.3	17.0	32.8	47.0
SO3031	Siderophore biosynthesis protein, putative	1.0	20.2	132.6	498.1
SO3032	Siderophore biosynthesis protein, putative	0.7	14.5	202.4	139.4
SO3033	Ferric alcaligin siderophore receptor	0.6	8.0	81.1	110.2
SO3344	Hypothetical protein	7.5	67.4	68.7	127.9
SO3667	Conserved hypothetical protein	0.8	17.7	121.6	130.9
SO3668	Conserved hypothetical protein	0.8	11.5	58.2	77.5
SO3669	Heme transport protein (HugA)	1.3	37.8	174.0	199.5
SO3670	TonB1 protein (TonB1)	6.2	79.7	155.2	225.3
SO3671	TonB system transport protein ExbB1 (ExbB1)	3.3	180.7	379.0	567.6
SO3672	TonB system transport protein ExbD1 (ExbD1)	2.4	55.1	108.8	175.5
SO3673	Hemin ABC transporter, periplasmic hemin-binding protein (HmuT)	1.5	34.6	104.4	83.2
SO3674	Hemin ABC transporter, permease protein (HmuU)	1.5	24.3	60.2	70.4
SO3675	Hemin ABC transporter, ATP-binding protein (HmuV)	1.2	39.9	104.1	111.3
SO3914	TonB-dependent receptor, putative	0.4	10.4	47.6	38.1
SO4636	Lipoprotein, putative	13.7	53.3	75.5	62.3

[a] Relative gene expression is presented as the mean ratio of the fluorescence intensity of $SrCl_2$-exposed cells to that of control cells. Each gene showed significant differential expression ($P < 0.05$) at a minimum of one time point. The time in minutes is that at which cells were harvested for RNA isolation following addition of 180 mM $SrCl_2$ to the experimental culture.

annotated as *czcA* family members with putative heavy metal efflux pump functions; energy metabolism genes, such as SO4606 and SO4607, which encode cytochrome *c* oxidase subunits II and I, respectively; and genes for putative transporters, such as KtrA (SO4281) and KtrB (SO4282) for potassium uptake, as well as genes possibly involved in osmotic stress protection (e.g., SO2923, which encodes a putative sodium/glutamate symporter).

The majority of differentially expressed genes grouped within cluster IV (1,205 genes), which comprised approximately two-thirds of the total number of genes displaying significant changes ($P < 0.05$ and $\geq$2-fold) in transcription at least at one time point during application of $SrCl_2$ stress. Genes involved in sulfate/thiosulfate uptake and sulfur metabolism showed coregulated expression patterns and clustered tightly in subgroup C of cluster IV (Fig. 2). A number of these genes displayed a distinct temporal pattern characterized by induction peaks at either 30 or 60 min poststress followed by a decrease in transcript abundance at 90 min (Table 3). For example, genes encoding an adenylylsulfate kinase (*cysC*), two hypothetical proteins (SO3724 and SO3725), and sulfate adenylyltransferase subunits (*cysN* and *cysD*) showed little change in expression 5 min after $SrCl_2$ addition and approximately threefold-greater expression in $SrCl_2$-shocked cells after 30 and 60 min followed by approximately two- to threefold repression at the 90-min time point. SO3724 and SO3725 en-

TABLE 2. Percentages of genes that showed similar expression profiles for the different gene functional categories following cluster analysis

Functional category	Cluster[a]								Genome[a]
	I	II	III			IV			
			A	B	C	D	E	F	
Amino acid biosynthesis			4.3	4.6	2.5	1.8	3.0	1.0	1.8
Biosynthesis of cofactors, prosthetic groups, and carriers				0.8	3.3	3.5	2.1	4.5	2.4
Cell envelope	5.9	7.1	4.3	2.3	2.9	3.1	2.1	4.0	3.5
Cellular processes			8.5	3.8	3.3	3.1	4.5	4.2	5.4
Central intermediary metabolism				1.5	2.9	0.4	0.6	1.3	1.2
DNA metabolism				3.1	2.0	2.2	2.7	2.2	2.9
Energy metabolism		21.4	2.1	4.8	4.5	4.8	5.9	15.4	6.1
Fatty acid and phospholipid metabolism				1.9	1.2	1.3	1.2	2.4	1.3
Hypothetical or conserved hypothetical	17.6	42.9	36.2	48.8	30.3	31.1	43.3	31.4	39.4
Mobile and extrachromosomal element functions				3.4	0.8	0.9	3.9	0.5	6.2
Protein fate			12.8	1.1	6.1	6.6	6.2	4.6	3.8
Protein synthesis				0.6	18.9	20.2	1.2	5.0	2.8
Purines, pyrimidines, nucleosides, and nucleotides		7.1		0.4	4.1	4.4	0.9	5.1	1.2
Regulatory functions		14.3	8.5	6.7			5.0	2.7	4.3
Signal transduction			0.0	1.9	1.6	1.8	0.9	1.1	1.8
Transcription			2.1	0.6	3.3	3.5	1.2	1.3	1.1
Transport and binding proteins	76.5		10.6	5.5	5.3	3.9	7.4	6.7	6.1
Unknown function		7.1	10.6	8.2	7.0	7.5	8.0	6.6	7.3

[a] Some genes are assigned to more than one functional category. Letters beneath clusters III and IV indicate subgroups.

TABLE 3. Subgroup C genes showing differences in temporal expression in response to strontium stress

Gene	Gene product	Mean ratio ($SrCl_2$/control) at[a]:			
		5 min	30 min	60 min	90 min
SO3599	Sulfate ABC transporter, periplasmic sulfate-binding protein (CysP)	1.2	3.5	3.5	0.4
SO3723	Adenylylsulfate kinase (CysC)	1.2	3.6	3.8	0.4
SO3724	Hypothetical protein	1.1	3.4	4.3	0.3
SO3725	Hypothetical protein	1.1	3.8	3.8	0.4
SO3726	Sulfate adenylyltransferase, subunit 1 (CysN)	0.9	2.7	3.4	0.3
SO3727	Sulfate adenylyltransferase, subunit 2 (CysD)	0.9	3.3	3.4	0.4
SO3736	Phosphoadenosine phosphosulfate reductase (CysH)	0.8	3.3	3.2	0.3
SO3737	Sulfite reductase (NADPH) hemoprotein beta-component (CysI)	1.0	3.8	3.3	0.3
SO3738	Sulfite reductase (NADPH) flavoprotein alpha-component (CysJ)	1.0	3.3	3.6	0.4
SO3819	Nitrogen regulatory protein, P-II	0.4	1.2	0.9	0.08
SO4026	Hypothetical protein	0.6	2.4	7.7	0.2
SO4410	Glutamine synthetase, type 1 (GlnA)	0.3	1.4	0.8	0.06
SO4654	Sulfate ABC transporter, permease protein (CysW-2)	0.8	2.8	5.9	0.6
SO4655	Sulfate ABC transporter, ATP-binding protein (CysA-2)	0.9	3.5	6.9	0.5

[a] Relative gene expression is presented as the mean ratio of the fluorescence intensity of $SrCl_2$-exposed cells to that of control cells. Each gene showed significant differential expression ($P < 0.05$) at a minimum of one time point. The time in minutes is that at which cells were harvested for RNA isolation following addition of 180 mM $SrCl_2$ to the experimental culture.

code hypothetical proteins and are positioned between *cysC* and *cysN* on the chromosome, suggesting that these poorly characterized genes may have functional roles in sulfur metabolism pathways. The gene region containing SO3736, SO3737, SO3738, and SO3739 showed similar expression patterns; its constituent genes encode a putative phosphoadenosine phosphosulfate reductase, two sulfite reductase components, and a hypothetical protein, respectively. A number of genes for expression of sulfate ABC transporter components (SO3599, SO4654, and SO4655) were within subgroup C, although some sulfate transporter members clustered in the adjacent subgroup D. The genes SO0929, SO2264, and SO2903, encoding putative *S*-adenosylmethionine synthetase, cysteine desulfurase, and cysteine synthase A proteins, were also found in subgroup D. In addition, a large number of genes encoding ribosomal proteins and other gene products involved in protein synthesis were found in subgroup D, which represented 20.2% of the subgroup, compared to 2.8% of the genome coding for proteins in this functional category.

A number of the 337 genes comprising subgroup E are associated with general and envelope stress responses. Examples of some of the gene products in this subgroup included transcriptional regulatory protein CpxR (encoded by SO4477) and its cognate sensor protein CpxA (encoded by SO4478), transcriptional regulatory protein KdpE (encoded by SO0059), RNA polymerase sigma-32 factor (encoded by SO4583), the sigma factor-70 ECF subfamily (encoded by SO1986), sigma-E factor regulatory proteins RseB (encoded by SO1344) and RseC (encoded by SO1345), chaperone proteins DnaJ (encoded by SO1127) and DnaK (encoded by SO1126), heat shock protein GrpE (encoded by SO1524), ClpB (encoded by SO3577), and proteases such as DegS (encoded by SO3943). The conserved hypothetical genes SO4650 and SO4651 also clustered in subgroup E and are located in a region of DNA directly upstream of SO4652 and SO4653, which showed similar coexpression patterns and encode members of a sulfate ABC transport system. The chromosomal location of SO4650 and SO4651 and the coexpression data implicate the corresponding conserved hypothetical proteins in sulfur transport or metabolism.

The largest node within cluster IV, designated as subgroup F, contained 624 genes that were mostly repressed and represented approximately one-third of the total number of differentially expressed genes. Subgroup F, like subgroups B and E, contained genes that represented each functional category. Genes whose products are annotated as being involved in energy metabolism constituted 15.4% of the subgroup, compared to 6.1% of the genome (Table 2). Genes in the functional category for purines, pyrimidines, nucleosides, and nucleotides also appeared to be slightly overrepresented in subgroup F (5.1%, compared to 1.2% of the genome) and were followed in terms of representation level by genes in the category for biosynthesis of cofactors, prosthetic groups, and carriers (5.8%, compared to 2.4% of the genome). Repressed genes in this cluster included those coding for such enzymes as cytochrome *c* oxidase (*ccoPQON* [SO2361 to SO2364]), menaquinone-specific isochorismate synthase (putative, SO4713), ubiquinone/menaquinone biosynthesis methyltransferase (*ubiE* [SO4199]), quinone-reactive Ni/Fe hydrogenase (*hoxK* [SO2099]), decaheme cytochrome *c* (*mtrA* [SO1777], *mtrB* [SO1776], *omcA* [SO1779], and *omcB* [SO1778]), NADH: ubiquinone oxidoreductase (*nqrABCDEF-2* [SO1103 to SO1108]), ornithine decarboxylase (*speF* [SO0314]), uroporphyrinogen-III synthase (*hemD* [SO4314]), ATP synthase F1 (*atpCDGAH* [SO4746 to SO4750]), ATP synthase F0 (*atpFEB* [SO4751 to SO4753]), succinate dehydrogenase (*sdhAB* [SO1928 and SO1929]), phosphoenolpyruvate carboxykinase (*pckA* [SO0162]), acetyltransferase (SO1936), and numerous ribosomal proteins. Genes with predicted functions in cellular detoxification were also repressed in response to $SrCl_2$ stress and clustered with energy metabolism genes as follows: outer membrane efflux family protein (putative, SO0518), cation efflux protein (putative, SO0519), and heavy metal efflux pump (CzcA family gene, SO0520).

Validation of microarray data by real-time RT-PCR. To independently confirm microarray transcriptome profiling, the

expression levels for four selected genes encoding two hypothetical proteins (SO0403, SO3062), a putative siderophore biosynthesis protein (SO3032), and a hemin ABC transporter (*hmuV*) were determined by real-time RT-PCR using the same cellular RNA samples analyzed by microarray hybridization. The genes selected for comparative real-time RT-PCR analysis displayed a range of up- and down-regulated expression patterns based on microarray analysis. A Pearson correlation coefficient derived from microarray-based gene expression measurements and real-time RT-PCR determinations for the four genes (SO0403, SO3032, SO3062, and *hmuV*) at postshock time intervals of 30, 60, and 90 min indicated a high level of concordance between the two datasets ($r^2 = 0.86$; $P = 0.0003$).

Increased $SrCl_2$ sensitivity by an *S. oneidensis* mutant defective in siderophore biosynthesis. To further investigate the possible physiological role of siderophore biosynthesis in Sr tolerance, the SO3032 gene within the putative siderophore biosynthesis operon, *alcA*-SO3031-SO3032, was inactivated by integration of the suicide plasmid pKNOCK-Km^r (2 kb in size) into the chromosomal SO3032 locus. Based on the genome sequence annotation of MR-1, SO3032 encodes a putative siderophore biosynthesis protein (18). Disruption of the SO3032 gene by suicide plasmid integration was verified by PCR amplification using SO3032-specific primers that flanked the pKNOCK-Km^r insertion sites. Siderophore production by the DSP10 parental strain, a *fur* deletion mutant (FUR2 [51]), the SO3032::pKNOCK mutant, and a SO3034::pKNOCK mutant defective in a putative ferric iron reductase (see Materials and Methods for details) was qualitatively compared using the chrome azurol S (CAS) agar plate assay (44). The ferric iron reductase encoded by SO3034 is presumably involved in the intracellular reduction of the internalized siderophore-associated ferric iron. CAS reactivity (siderophore production) was demonstrated by DSP10, FUR2, and the SO3034::pKNOCK mutant but not by the SO3032::pKNOCK mutant (results not shown). Results of the CAS assay indicated a physiological role of the SO3032 protein in siderophore biosynthesis, as predicted by the sequence annotation.

When grown aerobically in LB medium supplemented with different $SrCl_2$ concentrations, the SO3032::pKNOCK mutant was approximately 5- to 10-fold more sensitive than the parental DSP10 strain and MR-1 to $SrCl_2$ concentrations of $\geq$50 mM, while end point turbidity measurements showed that the growth of the SO3032 mutant resembled that of the wild-type and parental strains in the absence of added metal (Fig. 3). Growth of the SO3034::pKNOCK mutant under similar conditions was comparable to that of DSP10 and MR-1 (Fig. 3), suggesting that inactivation of the putative ferric iron reductase gene does not measurably impair cellular tolerance to Sr.

Further physiological studies demonstrated the accumulation of fine white precipitates in cultures of MR-1, DSP10, and SO3034::pKNOCK in the presence of $SrCl_2$ (Fig. 4A [results shown only for MR-1]). This precipitate was particularly abundant at $SrCl_2$ concentrations of 50 and 100 mM after a 3-day incubation period at 30°C, although the onset of precipitate formation was observed less than 18 h following inoculation. Parallel experiments with uninoculated LB broth amended with 50 mM or 100 mM $SrCl_2$ (negative controls) failed to show systematic changes in aqueous Sr concentration over the 3-day period, indicating that precipitate formation was dependent on the presence of *S. oneidensis* cells. Interestingly, $SrCl_2$-containing LB broth inoculated with the SO3032::pKNOCK mutant strain displayed no detectable precipitate formation at any of the $SrCl_2$ concentrations examined, and cellular growth was substantially retarded compared to that of the wild-type strain (Fig. 4B).

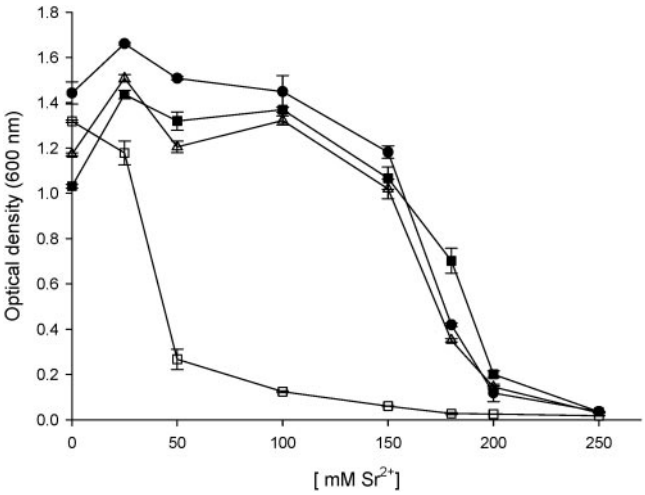

FIG. 3. Strontium resistance of wild-type and mutant strains of *S. oneidensis*. Dose-response curves are presented for wild-type MR-1 (■); parental DSP10 (●), a spontaneous rifampin-resistant derivative of *S. oneidensis* MR-1; the SO3032::pKNOCK insertion mutant (□); and the SO3034::pKNOCK insertion mutant (△). The means ± standard errors (bars) from three independent determinations are shown; three independent experiments were conducted.

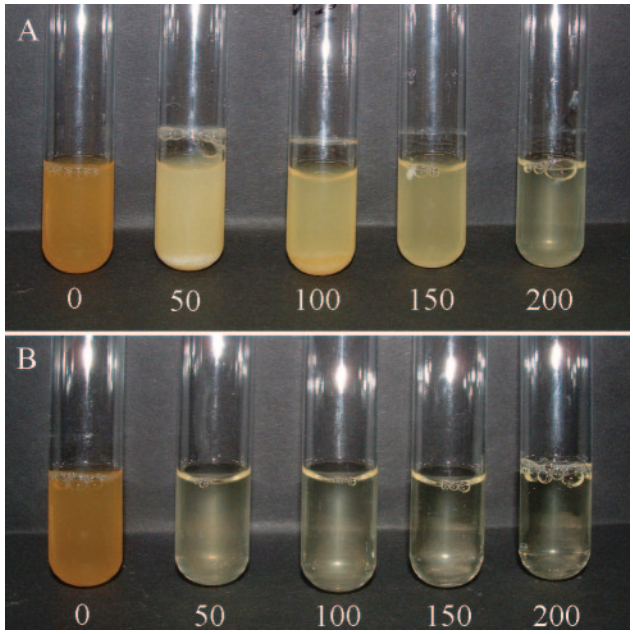

FIG. 4. Aerobic growth of *S. oneidensis* strains in the presence of different $SrCl_2$ concentrations over a 5-day period. (A) Growth of wild-type *S. oneidensis* MR-1 in LB medium; the different respective $SrCl_2$ concentrations (mM) are shown below the tubes. (B) Growth of the SO3032::pKNOCK insertion mutant in LB medium; the different respective $SrCl_2$ concentrations (mM) are shown below the tubes.

Spectrometric analyses of $SrCl_2$-exposed cells and milieu. Precipitate formation in liquid cultures of $SrCl_2$-treated MR-1 cells raised the question of whether Sr was being partitioned in solid-phase material under the growth conditions used. To investigate this possibility, LIBS was employed to analyze the elemental composition of the liquid milieu and that of the precipitate that formed during growth of wild-type *S. oneidensis* MR-1 in LB broth in the presence of $SrCl_2$. Figure 5 shows the emission spectra for elemental Sr in the dissolved and solid phases (Fig. 5B and C, respectively) in comparison to that for the LB-only background control (Fig. 5A). LIBS confirmed that the precipitate formed during aerobic growth of MR-1 in the presence of 50 mM $SrCl_2$ was particularly rich in Sr, with no other metals or counterions detected at similar levels of abundance (Fig. 5C). The Sr peaks are characteristic of their ionic transitions at 407.89 and 421.67 nm, and the ground state atomic emissions of Sr at 460.86 nm in precipitate (solid phase) and solution (dissolved phase) were observed. The emitted wavelengths are fingerprints for strontium metal, and all of the energy level transitions that occur in Sr via optical emission are recorded in the acquired spectra (Fig. 5). More Sr species (different energy level transitions) were observed in the solid phase than in the dissolved phase, in part because the liquid phase spread out over the entire filter, whereas the precipitate remained localized to the particular area upon which it was deposited.

Static SIMS was also used to examine the atomic and small-molecular-fragment ions in solid-phase material and/or in association with MR-1 following a 24-h growth of *S. oneidensis* in LB medium containing $SrCl_2$. We compared static SIMS mass spectra of freeze-dried *S. oneidensis* MR-1 cells grown aerobically either in the absence of added $SrCl_2$ (Fig. 6A) or in the presence of 150 mM $SrCl_2$ as a stressor (Fig. 6B; see Materials and Methods for details). The most intense peaks identified were within the range from 0 to 40 atomic mass units (amu) and corresponded to H, C, Na, and K. The distributions of these major cellular matrix elements were similar for both untreated and $SrCl_2$-treated cells (Fig. 6). In the case of $SrCl_2$-treated MR-1 cells (Fig. 6B), additional intense mass peaks were observed between 80 and 150 amu; these peaks were not present in the mass spectra for untreated control cells (Fig. 6A) or the pure $SrCl_2$ reference sample (data not shown). Peaks observed at 88 amu can be attributed to Sr^+ ions, while the absence of a peak at 89 amu ($^{88}Sr^+$ plus $^1H^+$) suggests the lack of hydrate formation at the sample surface. Other major mass peaks indicated the association of SrCO (116 amu), $SrCO_2$ (132 amu), and $SrCO_3$ (148 amu) species with MR-1 cells (Fig. 6B). Such $SrCO_n$ species were not detected in the spectra obtained for untreated control cells or pure $SrCl_2$ powder. Static SIMS analysis of wild-type cells grown in the presence of 50 mM $SrCl_2$ also indicated the association of Sr with MR-1 cells (data not shown).

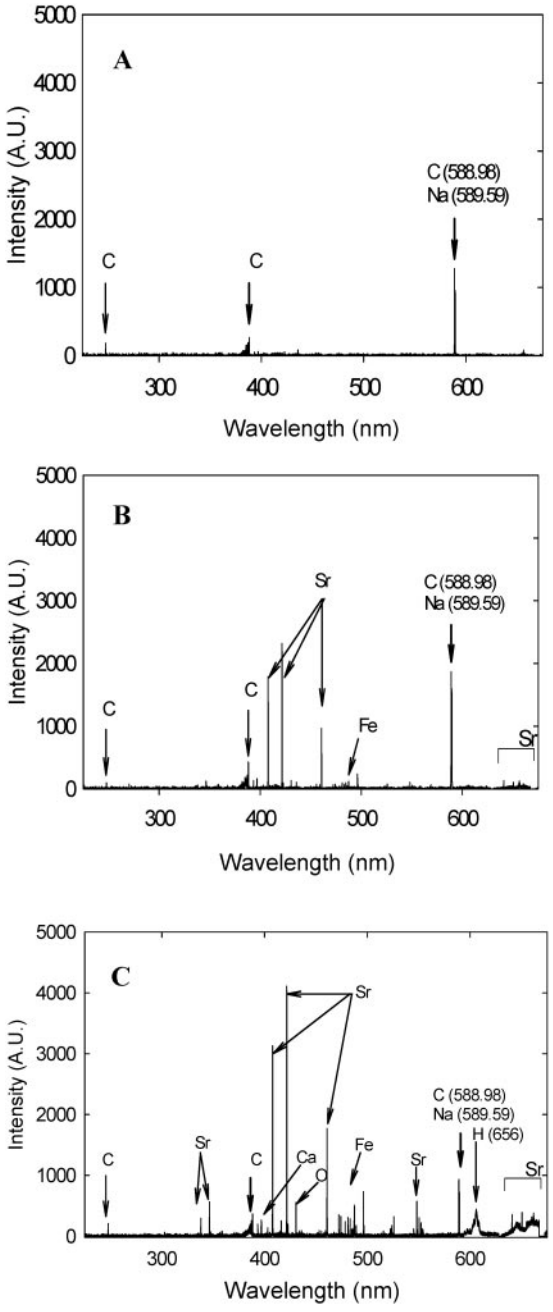

FIG. 5. Elemental analysis. LIBS was used to analyze the elemental composition of (A) liquid LB medium alone (background sample), (B) 0.2 ml of liquid (cell free) from an inoculated 50 mM $SrCl_2$ culture, and (C) 0.2 ml of precipitate material from an inoculated 50 mM $SrCl_2$ culture. Prior to elemental analysis, the precipitate (C) was washed twice in 50 mM Tris-Cl buffer (pH 7.0). Duplicate samples were analyzed by use of the LIBS technique in triplicate. Representative spectra are presented with the same vertical full scale.

DISCUSSION

The earth alkaline metal Sr is a common groundwater contaminant found at DOE field sites and was demonstrated in this study to exert a severe toxic effect on *S. oneidensis* growth at concentrations above 180 mM (Fig. 1). However, little is known about the biological impact of Sr toxicity on microbial systems or the underlying molecular mechanisms enabling resistance against Sr ions. To understand the molecular response to $SrCl_2$ and screen for genes potentially involved in Sr tolerance, we investigated global differential gene expression in *S. oneidensis* MR-1 in response to an acute exposure of a sublethal $SrCl_2$ concentration (180 mM). The transcriptomic exam-

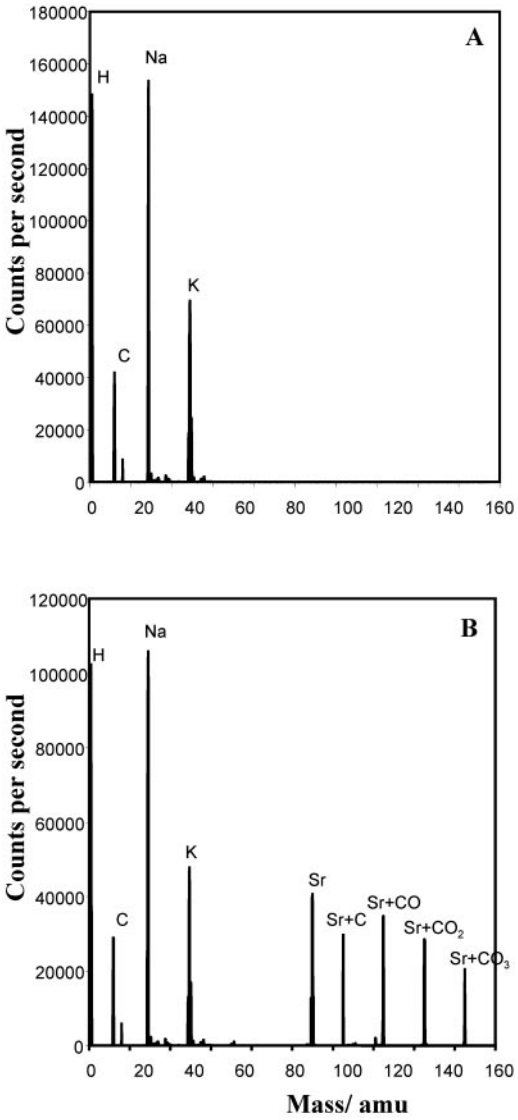

FIG. 6. Characterization of the chemical environment at the MR-1 cell surface by use of static SIMS. Comparison of static SIMS mass spectra of freeze-dried samples of *S. oneidensis* MR-1 cells grown aerobically for 24 h in LB medium (A) without added $SrCl_2$ (untreated sample) and (B) with 150 mM $SrCl_2$ (treated sample). Identified atoms/molecules are indicated above their respective peaks.

ination led to the observation that in *S. oneidensis*, nonradioactive Sr stress results in the high-level induction of a number of genes that code for proteins involved in siderophore-mediated iron sequestration and transport, e.g., TonB-dependent receptor genes (SO1482, SO3914), *hmuTUV*, *alcA*-SO3031-SO3032, *hugA*-SO3668-SO3667, and *tonB1-exbB1-exbD1*. The up-regulation of *S. oneidensis* genes encoding the synthesis of iron chelators and iron uptake systems in Sr-stressed cells occurred despite the fact that the growth medium (LB) contained an amount of iron sufficient to permit low-level expression or repression of these genes in nonstressed cells. In contrast to results from this study and a transcriptome experiment in which MR-1 cells were grown to mid-exponential stage in the presence of 180 mM $SrCl_2$ (Brown et al., unpublished data), the expression levels for MR-1 siderophore biosynthesis genes (*alcA*-SO3031-SO3032) and other iron-responsive genes were either up-regulated at modest levels (approximately two- to fivefold) or found not to be significantly changed ($P = 0.05$) in response to elevated NaCl conditions (25), suggesting that the high induction levels observed for iron-binding and transport genes in the present study could not be attributed, in any large part, to the chloride anion.

Overall, enhancing the expression of iron-binding proteins and transporters appeared to constitute the predominant transcriptomal response of *S. oneidensis* to Sr shock. However, it is not clear whether induction of siderophore biosynthetic and iron transport genes was a direct consequence of intracellular iron limitation, an indirect effect of $SrCl_2$ interfering with the Fur (ferric uptake regulator) protein leading to derepression of the iron regulon, or a strategy for sequestering Sr via siderophore complexation. Mn^{2+} resistance has been used as a selection strategy to obtain *fur* mutants in several bacteria (12, 16, 39), and the Fur-binding site for regulatory active Fe^{2+} may be occupied in vitro by Co^{2+}, Mn^{2+}, or other divalent cations (17), raising the possibility that intracellular Sr^{2+} may interfere with normal Fur function. Iron-chelating siderophores from other microorganisms have been shown to bind other metals, such as thorium, uranium, vanadium, and plutonium (3, 8, 20, 40, 47). One possibility is that *S. oneidensis* cells were unable to increase cellular iron upon exposure to $SrCl_2$ because the competition of Sr with iron for specific binding sites in iron-sensing proteins or siderophores led to high expression levels for iron acquisition genes. Alternatively, the effective complexation of iron by high-affinity iron chelators may be negatively impacted by changes in the ionic strength of the growth medium, due to excess Sr. The indirect effects of environmental stresses on an adequate iron supply for the cell have been observed elsewhere (19, 49). Hoffmann et al. (19), for example, found that high salinity caused iron limitation in *Bacillus subtilis*, thereby initiating derepression of certain iron-regulated genes. This pattern of derepression, furthermore, could be largely reversed by the addition of excess $FeCl_3$ to the salt-containing medium (19). Similarly, cobalt tolerance in yeast cells was dependent on the cellular iron content (49). If *S. oneidensis* cells stressed by Sr experienced an iron deficiency, we would predict that the growth inhibition exhibited by these cultures should be at least partially compensated for by the addition of excess iron to the growth medium. However, we did not observe increased tolerance of MR-1 cells to 180 mM $SrCl_2$ in the presence of added external $FeCl_3$ (results not shown). Further research is needed to determine the extent to which Sr stress and iron limitation in *S. oneidensis* are linked at physiological and molecular levels.

In addition to the induction of iron-binding and transport genes noted above, microarray analysis revealed changes in the mRNA abundance of genes encoding components in sulfate transport and assimilation pathways. Inorganic sulfate is reduced and incorporated into bioorganic compounds via a pathway termed assimilatory sulfate reduction, which is the major route of cysteine biosynthesis in most microorganisms (reviewed in references 23 and 24). Expression levels of genes with putative functions in sulfate transport/uptake (SO3599, SO4654, and SO4655), sulfate activation (SO3723, SO3726, and SO3727), and reduction (SO3736, SO3737, and SO3738)

peaked at either the 30- or the 60-min time point and then were repressed 1.7- to 3.3-fold after 90 min into $SrCl_2$ treatment (Table 3). These open reading frames clustered tightly together in subgroup C of cluster IV (Fig. 2), suggesting that their expression is coregulated in response to high $SrCl_2$ concentrations. Two genes (SO3724 and SO3725) encoding hypothetical proteins also displayed a similar temporal expression pattern and clustered within subgroup C (Table 2). These unknown genes are located in close proximity between SO3723 (*cysC*) and SO3726 (*cysN*) in the MR-1 genome and transcribed in the same direction as the neighboring *cys* genes, which suggests the likelihood that the products of these unknown genes are also involved in assimilative sulfur metabolism. MR-1 gene products presumed to be responsible for the activation of the serine acceptor and the incorporation of sulfide into *O*-acetylserine to form cysteine exhibited either no change or a decrease in transcription, based on microarray analysis.

Cellular metabolic activities can lead to the precipitation of metals, either directly through microbially catalyzed redox reactions (7) or indirectly through the production and secretion of reactive inorganic ligands (e.g., sulfide, phosphate, or inorganic carbon) (38). Cunningham and Lundie (6), for example, reported that *Clostridium thermoaceticum* cells could tolerate up to at least 2 mM cadmium by producing sulfide, which formed an insoluble precipitate with the metal. Alternatively, biosynthesis of the chemically undefined MR-1 siderophore (production of which is predicted to be encoded at least in part by the *alcA*-SO3031-SO3032 operon) may be dependent on the availability of assimilable sulfur, which is required for sufficient intracellular pools of cysteine. Pyochelin biosynthesis in *Burkholderia cenocepacia* has been shown to be sensitive to sulfur availability (11). The high induction levels in transcription of the *S. oneidensis* siderophore biosynthesis operon in response to $SrCl_2$ (Table 1) may result in an increased cellular demand for sulfur, which, in turn, results in the up-regulation of genes involved in sulfate transport and utilization.

Active extrusions of heavy metal ions from the cell via P-type ATPase efflux systems or chemiosmotic efflux pumps are mechanisms of heavy metal resistance (reviewed in reference 37), and plasmid-determined cadmium and chromate efflux in *Pseudomonas* species has been demonstrated (2, 22). In this study, the expressions of heavy metal efflux genes, such as those encoding CzcA family efflux pumps, were repressed or showed only modest increases, suggesting that at the transcriptional level these genes did not play a major role in the molecular response of MR-1 to Sr. However, we cannot rule out the possibility that these genes are constitutively expressed or regulated at the level of translation. Several other efflux genes, such as SO2045, which encodes a putative cation efflux family protein, did show increased transcript abundance over the time course of Sr exposure.

Our results demonstrated that growth of *S. oneidensis* MR-1 supports solid-phase partitioning of Sr ions and that Sr precipitation was dependent on a functional siderophore biosynthesis operon (*alcA*-SO3031-SO3032). Both qualitative LIBS and static SIMS confirmed that *S. oneidensis* MR-1 is capable of mediating the solid-phase capture of Sr, and metal precipitation likely constitutes the primary defense used by MR-1 cells to combat Sr toxicity. These findings are consistent with what has been observed for other *Shewanella* species (15, 38, 41, 46). Roden et al. (41), for example, found that under appropriate conditions Sr could be immobilized in siderite ($FeCO_3$) produced during Fe(III) oxide reduction by *Shewanella putrefaciens* strain CN32, and solid-phase capture of Sr was shown for *Shewanella alga* strain BrY (38). Whether siderophore synthesis directly contributes to the extracellular sequestration of Sr or indirectly enables Sr precipitation by promoting cell growth remains unclear. Future efforts will need to focus on purifying the endogenous *S. oneidensis* MR-1 siderophore, whose chemical structure is not known, and testing its binding affinity for Sr relative to those for Fe and other metals.

ACKNOWLEDGMENTS

We thank Ben Shneiderman and Jinwook Seo for making the HC3 software freely available and Craig Brandt for assistance in comparing the microarray and real-time RT-PCR data sets.

This work was part of the Virtual Institute for Microbial Stress and Survival (http://vimss.lbl.gov), supported by the U.S. Department of Energy, Office of Science, Office of Biological and Environmental Research, Genomics Program:GTL through contract DE-AC02-05CH11231 between Lawrence Berkeley National Laboratory and the U.S. Department of Energy. Oak Ridge National Laboratory is managed by University of Tennessee—Battelle LLC for the Department of Energy under contract DOE-AC05-00OR22725.

REFERENCES

1. **Alexeyev, M. F.** 1999. The pKNOCK series of broad-host-range mobilizable suicide vectors for gene knockout and targeted DNA insertion into the chromosome of gram-negative bacteria. BioTechniques **26:**824–828.
2. **Alvarez, A. H., R. Moreno-Sanchez, and C. Cervantes.** 1999. Chromate efflux by means of the ChrA chromate resistance protein from *Pseudomonas aeruginosa*. J. Bacteriol. **181:**7398–7400.
3. **Baysse, C., D. de Vos, Y. Naudet, A. Vandermonde, U. Ochsner, J.-M. Meyer, H. Budzikiewicz, M. Schäfer, R. Fuchs, and P. Cornelis.** 2000. Vanadium interferes with siderophore-mediated iron uptake in *Pseudomonas aeruginosa*. Microbiology **146:**2425–2434.
4. **Beveridge, T. J.** 1989. Role of cellular design in bacterial metal accumulation and mineralization. Annu. Rev. Microbiol. **43:**147–171.
5. **Cannon, D. M., Jr., N. Winograd, and A. G. Ewing.** 2000. Quantitative chemical analysis of single cells. Annu. Rev. Biophys. Biomol. Struct. **29:** 239–263.
6. **Cunningham, D. P., and L. L. Lundie, Jr.** 1993. Precipitation of cadmium by *Clostridium thermoaceticum*. Appl. Environ. Microbiol. **59:**7–14.
7. **Davis, J. A., D. B. Kent, B. A. Rea, A. S. Maest, and S. P. Garabedian.** 1993. Influence of redox environment and aqueous speciation on metal transport in groundwater, p. 223–273. *In* H. E. Allen, E. M. Perdue, and D. S. Brown (ed.), Metals in groundwater. Lewis Publishers, Chelsea, Mich.
8. **Durbin, P. W., N. Jeung, S. J. Rodgers, P. N. Turowski, F. L. Weitl, D. L. White, and K. N. Raymond.** 1989. Removal of 238Pu(IV) from mice by poly-catecholate, -hydroxamate or -hydroxypyridonate ligands. Radiat. Prot. Dosim. **26:**351–358.
9. **Eisen, M. B., P. T. Spellman, P. O. Brown, and D. Botstein.** 1998. Cluster analysis and display of genome-wide expression patterns. Proc. Natl. Acad. Sci. USA **95:**14863–14868.
10. **Eugster, O., J. T. Armstrong, and G. J. Wasserburg.** 1985. Ion process. Int. J. Mass Spectrom. **66:**291–312.
11. **Farmer, K. L., and M. S. Thomas.** 2004. Isolation and characterization of *Burkholderia cenocepacia* mutants deficient in pyochelin production: pyochelin biosynthesis is sensitive to sulfur availability. J. Bacteriol. **186:**270–277.
12. **Funahashi, T., C. Fujiwara, M. Okada, S. Miyoshi, S. Shinoda, S. Narimatsu, and S. Yamamoto.** 2000. Characterization of *Vibrio parahaemolyticus* manganese-resistant mutants in reference to the function of the ferric uptake regulatory protein. Microbiol. Immunol. **44:**963–970.
13. **Gadd, G. M.** 2000. Bioremedial potential of microbial mechanisms of metal mobilization and immobilization. Curr. Opin. Biotechnol. **11:**271–279.
14. **Gao, H., Y. Wang, X. Liu, T. Yan, L. Wu, E. Alm, A. Arkin, D. K. Thompson, and Z. Zhou.** 2004. Global transcriptome analysis of the heat shock response of *Shewanella oneidensis*. J. Bacteriol. **186:**7796–7803.
15. **Glasauer, S., S. Langley, and T. J. Beveridge.** 2001. Sorption of Fe (hydr)oxides to the surface of *Shewanella putrefaciens*: cell-bound fine-grained minerals are not always formed de novo. Appl. Environ. Microbiol. **67:**5544–5550.
16. **Hantke, K.** 1981. Regulation of ferric iron transport in *Escherichia coli* K12: isolation of a constitutive mutant. Mol. Gen. Genet. **182:**288–292.

17. **Hantke, K.** 2001. Iron and metal regulation in bacteria. Curr. Opin. Microbiol. **4:**172–177.
18. **Heidelberg, J. F., I. T. Paulsen, K. E. Nelson, E. J. Gaidos, W. C. Nelson, T. D. Read, J. A. Eisen, R. Seshadri, N. Ward, B. Methe, R. A. Clayton, T. Meyer, A. Tsapin, J. Scott, M. Beanan, L. Brinkac, S. Daugherty, R. T. DeBoy, R. J. Dodson, A. S. Durkin, D. H. Haft, J. F. Kolonay, R. Madupu, J. D. Peterson, L. A. Umayam, O. White, A. M. Wolf, J. Vamathevan, J. Weidman, M. Impraim, K. Lee, K. Berry, C. Lee, J. Mueller, H. Khouri, J. Gill, T. R. Utterback, L. A. McDonald, T. V. Feldblyum, H. O. Smith, J. C. Venter, K. H. Nealson, and C. M. Fraser.** 2002. Genome sequence of the dissimilatory metal ion-reducing bacterium *Shewanella oneidensis*. Nat. Biotechnol. **20:**1118–1123.
19. **Hoffmann, T., A. Schütz, M. Brosius, A. Völker, U. Völker, and E. Bremer.** 2002. High-salinity-induced iron limitation in *Bacillus subtilis*. J. Bacteriol. **184:**718–727.
20. **John, S. G., C. E. Ruggiero, L. E. Hersman, C. S. Tung, and M. P. Neu.** 2001. Siderophore mediated plutonium accumulation by *Microbacterium flavescens* (JG-9). Environ. Sci. Technol. **35:**2942–2948.
21. **Kalogeraki, V. S., and S. C. Winans.** 1997. Suicide plasmids containing promoterless reporter genes can simultaneously disrupt and create fusions to target genes of diverse bacteria. Gene **188:**69–75.
22. **Kawai, K., H. Horitsu, K. Hamada, and M. Watanabe.** 1990. Induction of cadmium resistance of *Pseudomonas putida* GAM-1. Agric. Biol. Chem. **54:**1553–1555.
23. **Kertesz, M. A.** 1999. Riding the sulfur cycle: metabolism of sulfonates and sulfate esters in Gram-negative bacteria. FEMS Microbiol. Rev. **24:**135–175.
24. **Kredich, N. M.** 1996. Biosynthesis of cysteine, p. 514–527. *In* F. C. Neidhardt, R. Curtiss III, E. C. C. Lin, K. B. Low, B. Magasanik, W. S. Reznikoff, M. Riley, M. Schaechter, and H. E. Umbarger (ed.), *Escherichia coli* and *Salmonella typhimurium*: cellular and molecular biology, 2nd ed. American Society for Microbiology, Washington, D.C.
25. **Liu, Y., W. Gao, Y. Wang, L. Wu, X. Liu, T. Yan, E. Alm, A. Arkin, D. K. Thompson, M. W. Fields, and J. Zhou.** 2005. Transcriptome analysis of *Shewanella oneidensis* MR-1 in response to elevated salt conditions. J. Bacteriol. **187:**2501–2507.
26. **Lovley, D.** 1991. Dissimilatory Fe(III) and Mn(IV) reduction. Microbiol. Rev. **55:**259–287.
27. **Lovley, D. R.** 2000. Environmental microbe-metal interactions. American Society for Microbiology, Washington, D.C.
28. **Lovley, D. R.** 1994. Microbial reduction of iron, manganese and other metals. Adv. Agron. **54:**175–231.
29. **Lovley, D. R., and E. J. P. Phillips.** 1992. Bioremediation of uranium contamination with enzymatic uranium reduction. Environ. Sci. Tech. **26:**2228–2234.
30. **Martin, M. Z., and M. D. Cheng.** 2000. The detection of chromium aerosol using time-resolved laser-induced plasma spectroscopy. Appl. Spectrosc. **54:**1279–1285.
31. **Mays, C. W., and R. D. Lloyd.** 1972. Bone sarcoma risk from 90Sr, p. 352–375. *In* M. Goldman and L. K. Bustad (ed.), Biomedical implications of radiostrontium exposure: proceedings. AEC Symposium Series 25, U.S. Department of Energy, Washington, D.C.
32. **Moser, D., and K. H. Nealson.** 1996. Growth of the facultative anaerobe *Shewanella putrefaciens* by elemental sulfur reduction. Appl. Environ. Microbiol. **62:**2100–2105.
33. **Myers, C. R., and K. H. Nealson.** 1988. Bacterial manganese reduction and growth with manganese oxide as the sole electron acceptor. Science **240:**1319–1321.
34. **Myers, C. R., and K. H. Nealson.** 1988. Microbial reduction of manganese oxides: interactions with iron and sulfur. Geochim. Cosmochim. Acta **52:**2727–2732.
35. **Myers, C. R., and K. H. Nealson.** 1990. Respiration-linked proton translocation coupled to anaerobic reduction of manganese(IV) and iron(III) in *Shewanella putrefaciens* MR-1. J. Bacteriol. **172:**6232–6238.
36. **Nealson, K. H., and D. A. Saffarini.** 1994. Iron and manganese in anaerobic respiration: environmental significance, physiology, and regulation. Annu. Rev. Microbiol. **48:**311–343.
37. **Nies, D. H.** 2003. Efflux-mediated heavy metal resistance in prokaryotes. FEMS Microbiol. Rev. **27:**313–339.
38. **Parmar, N., L. A. Warren, E. E. Roden, and F. G. Ferris.** 2000. Solid phase capture of strontium by the iron reducing bacteria *Shewanella alga* strain BrY. Chem. Geol. **169:**281–288.
39. **Prince, R. W., C. D. Cox, and M. L. Vasil.** 1993. Coordinate regulation of siderophore and exotoxin A production: molecular cloning and sequencing of the *Pseudomonas aeruginosa fur* gene. J. Bacteriol. **175:**2589–2598.
40. **Raymond, K. N., G. E. Freeman, and M. J. Kappel.** 1984. Actinide-specific complexing agents: their structural and solution chemistry. Inorg. Chim. Acta **94:**193–204.
41. **Roden, E. E., M. R. Leonardo, and F. G. Ferris.** 2002. Immobilization of strontium during iron biomineralization coupled to dissimilatory hydrous ferric oxide reduction. Geochim. Cosmochim. Acta **66:**2823–2839.
42. **Sambrook, J., E. F. Fritsch, and T. Maniatis.** 1989. Molecular cloning: a laboratory manual, 2nd ed. Cold Spring Harbor Laboratory Press, Cold Spring Harbor, N.Y.
43. **Schena, M., D. Shalon, R. Heller, A. Chai, P. O. Brown, and R. W. Davis.** 1996. Parallel human genome analysis: microarray-based expression monitoring of 1000 genes. Proc. Natl. Acad. Sci. USA **93:**10614–10619.
44. **Schwyn, B., and J. B. Neilands.** 1987. Universal chemical assay for the detection and determination of siderophores. Anal. Biochem. **160:**47–56.
45. **Small, T. D., L. A. Warren, and F. G. Ferris.** 2001. Influence of ionic strength on strontium sorption to bacteria, Fe(III) oxide, and composite bacteria-Fe(III) oxide surfaces. Appl. Geochem. **16:**939–946.
46. **Small, T. D., L. A. Warren, E. E. Roden, and F. G. Ferris.** 1999. Sorption of strontium by bacteria, Fe(III) oxide, and bacteria-Fe(III) oxide composites. Environ. Sci. Technol. **33:**4465–4470.
47. **Smith, W. L., and K. N. Raymond.** 1981. Specific sequestering agents for the actinides. 6. Synthetic and structural chemistry of tetrakis(N-alkylalkanehydroxamato)thorium(IV) complexes. J. Am. Chem. Soc. **103:**3341–3349.
48. **Spencer, H., D. Laszol, and M. Brothers.** 1957. Strontium85 and calcium45 metabolism in man. J. Clin. Investig. **36:**680–688.
49. **Stadler, J. A., and R. J. Schweyen.** 2002. The yeast iron regulon is induced upon cobalt stress and crucial for cobalt tolerance. J. Biol. Chem. **277:**39649–39654.
50. **Thompson, D. K., A. S. Beliaev, C. S. Giometti, S. L. Tollaksen, T. Khare, D. P. Lies, K. H. Nealson, H. Lim, J. Yates III, C. C. Brandt, J. M. Tiedje, and J. Zhou.** 2002. Transcriptional and proteomic analysis of a ferric uptake regulator (Fur) mutant of *Shewanella oneidensis*: possible involvement of Fur in energy metabolism, transcriptional regulation, and oxidative stress. Appl. Environ. Microbiol. **68:**881–892.
51. **Wan, X.-F., N. C. VerBerkmoes, L. A. McCue, D. Stanek, H. Connelly, L. J. Hauser, L. Wu, X. Liu, T. Yan, A. Leaphart, R. L. Hettich, J. Zhou, and D. K. Thompson.** 2004. Transcriptomic and proteomic characterization of the Fur modulon in the metal-reducing bacterium *Shewanella oneidensis*. J. Bacteriol. **186:**8385–8400.